1998-01

A young lens of Red Sea Water in the Arabian Sea

Meschanov, SL

10.1016/s0967-0637(97)00018-6
Deep Sea Research Part I: Oceanographic Research Papers
Elsevier BV

Pergamon

DEEP-SEA RESEARCH
PART I

Deep-Sea Research I 45 (1998) 1–13

A young lens of Red Sea Water in the Arabian Sea

S.L. Meschanov, G.I. Shapiro

P.P. Shirshov Institute of Oceanology, 23 Krasikova Street, 117218 Moscow, Russia

Received 4 April 1995; received in revised form 24 June 1996; accepted 12 November 1996

Abstract

CTD data collected in March–April 1980 in the Arabian Sea during the 22nd cruise of *R.V. Akademik Vernadsky* were used to investigate the structure and dynamics of a young lens of Red Sea Water (Reddy) in the initial stage of its formation. The core of the young lens with maximum temperature of 11.07°C and maximum salinity of 35.56 was located at depths of 640–830 m, and had temperature and salinity anomalies of 0.75°C and 0.22 with respect to the background water. The lens core, of thickness of 190 m, was connected to the main Red Sea Water tongue by a thin layer with vertical extent of about 20 m. In contrast to Meddies frequently observed in the North Atlantic, the density anomaly of the Reddy did not exceed $0.04\,kg\cdot m^{-3}$. A trajectory of the lens movement was reconstructed. The dynamic impact of a deep-reaching cyclonic meander on the large-scale tongue of Red Sea Water resulted in the Reddy formation near 16°N, 61°E and its subsequent movement to the south over a distance of about 370 km.

1. Introduction

High-salinity Red Sea Water (RSW) flows out of the Red Sea through the shallow Strait of Bab el Mandeb and propagates eastward in the Gulf of Aden, mainly at depths of 400–700 m. Further east in the Arabian Sea the dense RSW sinks to depths of 600–900 m and is revealed in vertical profiles as a relative salinity maximum with a salinity of 35.5–35.7, temperature of 11°C, and density σ_t ranging between 27.15 and $27.35\,kg\cdot m^{-3}$ (Rochford, 1964; Sabinin, 1964). In winter the intensity of RSW outflow through the Strait reaches $0.57\times10^6\,m^3\cdot s^{-1}$ (Patzert, 1974), and is 10 times higher than in summer (Maillard and Soliman, 1986) due to the effect of the monsoon wind stress. Nevertheless, because of the very large volume of RSW in the Indian Ocean, evaluated as $2.4\times10^{14}\,m^3$, seasonal variations of outflow do not significantly influence the seasonal variability of the RSW spatial distribution in the Arabian Sea. The seasonal variations of the RSW distribution reflect the main features of surface water

0967-0637/98/$19.00
PII: S0967-0637(97)00018-6

circulation: the preferentially southward transport of the RSW along the Somali coast occurs in winter (the north-east monsoon), whereas the eastward spreading is intensified in summer, during the south-west monsoon Gamsakhurdia *et al.* (1991).

Along with seasonal changes, there is a strong synoptic-scale variability of the north-west Indian Ocean circulation. It was in the Arabian Sea, that synoptic-scale eddies of the open ocean were discovered for the first time during the *POLYGON-67* experiment (Koshlyakov *et al.*, 1970).

Mesoscale structure and spreading of RSW in the Arabian Sea were examined by Shapiro and Meschanov (1991) [hereafter referred to as SM (1991)] on the basis of a hydrographic data set collected between 1935 and 1981. It was noted that the spreading of RSW occurs partially as high-salinity, isolated patches (lenses), some of which also have positive temperature anomalies. Seven RSW lenses were identified, and were called "Reddies" (Red Sea eddies) in accordance with W. Zenk's suggestion.

Isolated lenses of RSW in the Indian Ocean have some features in common with the Mediterranean Water lenses (Meddies) frequently observed in the North Atlantic. Both result from warm, salty outflows, and both have anomalous characteristics compared to the background. Reddies and Meddies are of the same horizontal (about 100 km) and vertical (a few hundred meters) scales. At the same time, there is a significant difference between Reddies and Meddies. Meddies are characterized by a strong density anomaly ($\Delta\sigma_t \geqslant 0.1\ \mathrm{kg \cdot m^{-3}}$) that leads to high azimuthal velocities. The Reddies reported by SM (1991) were almost undetectable in the density field. Another different feature is the direction of salty water outflow. Mediterranean Water in the Gulf of Cadiz spreads mainly westward, while the tongue of RSW in the Gulf of Aden propagates mainly eastward. This means that for Meddies the westward self-propagation velocity due to the β-effect (Nof, 1982; Shapiro, 1984) is in the same direction as the spreading of Mediterranean Water, whereas for Reddies it is in the opposite direction to the large-scale spreading of Red Sea Water.

A number of mechanisms for Meddy formation were proposed. Numerical process studies demonstrated the possibility of Meddy formation in the Iberian Basin by baroclinic instability of a northward jet of Mediterranean Water and by fragmentation of large-scale Mediterranean water blobs (Käse *et al.*, 1989). The formation of a Meddy in the region off Cape St. Vincent was observed by Bower *et al.* (1995). A detailed description of another newly formed Meddy found in the Gulf of Cadiz was given by Prater and Sanford (1994). A mesoscale experiment in the Azores–Madeira region revealed an interaction of the large-scale salt tongue of Mediterranean Water and synoptic-scale subsurface meanders of the Azores Current. It was suggested that bursts of cold subpolar water carried by the meanders interact strongly with westward pulses of salty Mediterranean Water to cause the salt tongue to become unstable and produce Meddies (Käse and Zenk, 1987).

With Reddies, there is no exact information about physical mechanisms, places of origin and decay, dynamics or possible trajectories. In this paper we describe a Reddy at the stage of its generation using observational data. We analyse the distribution of several passive tracers in order to determine the place of its origin and the role of the largescale and mesoscale flow field in its dynamics.

2. Methods

The paper is based on CTD data gathered in the Arabian Sea on the 22nd cruise of *R.V. Akademik Vernadsky*. Measurements were carried out during the onset of the south-west monsoon (March–April 1980) within the region 10–17°N, 58–68°E (Fig. 1). The study area was covered by a grid of 117 CTD stations with a nominal spacing of 72 km zonally and 111 km meridionally (Fig. 2). The grid was fine enough to identify

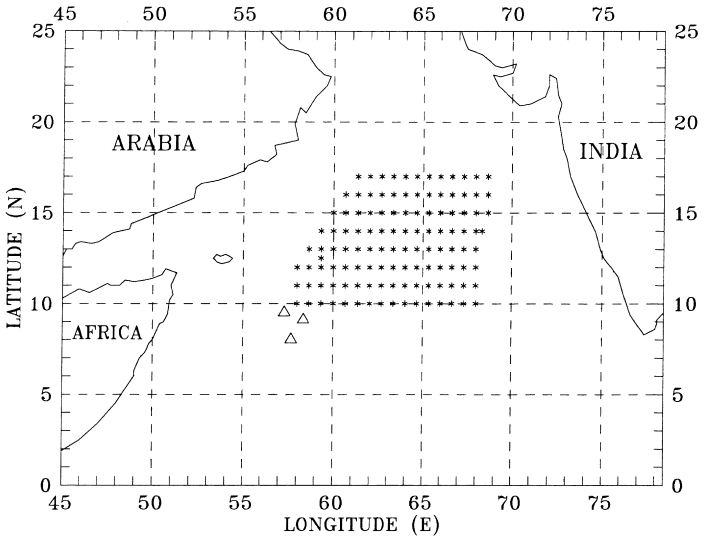

Fig. 1. CTD survey of *R.V. Akademik Vernadsky* cruise Number 22 in spring 1980. Positions of moorings are given by triangles.

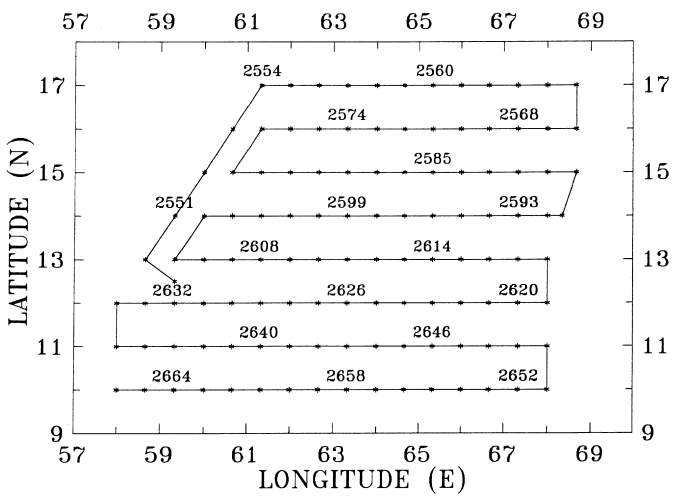

Fig. 2. The *R.V. Akademik Vernadsky* cruise Number 22 track with CTD stations numbers.

mesoscale features but too coarse to resolve their detailed structure. The survey was completed over a period of three weeks and may be considered as a quasi-synoptic. Measurements were carried out by an *ISTOK-4* CTD-profiler from the ocean surface down to 1750 m, with 5 m vertical resolution, which is sufficient for an adequate description of the RSW structure. Vertical profiles of temperature and salinity were supplemented at depths 2000, 2500, 3000, 3500 and 4000 m by monthly mean (March) values deduced from "Tables of monthly and annual temperature and salinity standards in the Indian Ocean", published by VNIIGMI-World Data Centre (Obninsk, Russia) in 1981. For the present research we restrict ourselves to the area 10–17°N, 60°00′–64°40′E which is covered by 61 hydrographic stations.

Following Rochford (1964), an analysis of T–S diagrams and vertical profiles was carried out to reveal the intermediate salinity maxima related to the Red Sea Water in the σ_t range 27.15–27.35 $kg \cdot m^{-3}$. The instrumental (relative) accuracy of the *ISTOK-4* profiler was 0.01°C for temperature and 0.02 for salinity. Because of this, only salinity inversions of 0.04 or greater were taken into account. To filter out the distortions of the thermohaline fields due to internal waves, we performed the analysis of the RSW spatial structure using the salinity distribution on the isopycnal surface $\sigma_t = 27.25\ kg \cdot m^{-3}$.

3. Results

The distribution of salinity on the isopycnal surface $\sigma_t = 27.25\ kg \cdot m^{-3}$ (a depth range of 650–750 m) is shown in Fig. 3. High-salinity RSW (with $S > 35.5$) interacts with the low-salinity intermediate water mass of the Arabian Sea (with $S < 35.3$). The leading edge of the large-scale RSW tongue (marked by 35.5 isohaline) is jagged and broken up into synoptic-scale meanders. The meander located at 61–63°E almost breaks off the main RSW tongue, and a salt patch of RSW can be easily seen in Fig. 3. The salt patch does not detach completely from the main tongue, but is connected to it by a salty layer with a vertical extent of about 20 m (Fig. 4a), which is very thin compared to the total vertical extent of the patch (190 m). For this reason we can specify this almost isolated patch as a young lens, or Red Sea eddy. Three adjacent oceanographic stations were occupied inside the Reddy (Fig. 3). Therefore, defined as having salinity greater than 35.5, the Reddy core has a horizontal scale of at least 110 km in the north–south direction and at least 70 km east–west. Analysis of temperature and salinity distributions on the isopycnal surface $\sigma_t = 27.25\ kg \cdot m^{-3}$ shows that the characteristic of the salt patch is close to that found in the north-west corner of the survey, and the salinity distribution on the isopycnal surface is a good tracer of the young Reddy movement.

Zonal sections of salinity, temperature and density σ_t through the Reddy are shown in Fig. 4. The lens core with $S > 35.5$ is clearly observed in the salinity section. It is less visible in the temperature section as a local patch of relatively warm water with $T > 11$°C and is almost undetectable in the density section. This situation is common for the RSW lenses observed earlier in the Arabian Sea (SM, 1991). The isopycnals in the Reddy do not bow up (upper half) and down (lower half) as in Meddies (Fig. 4c).

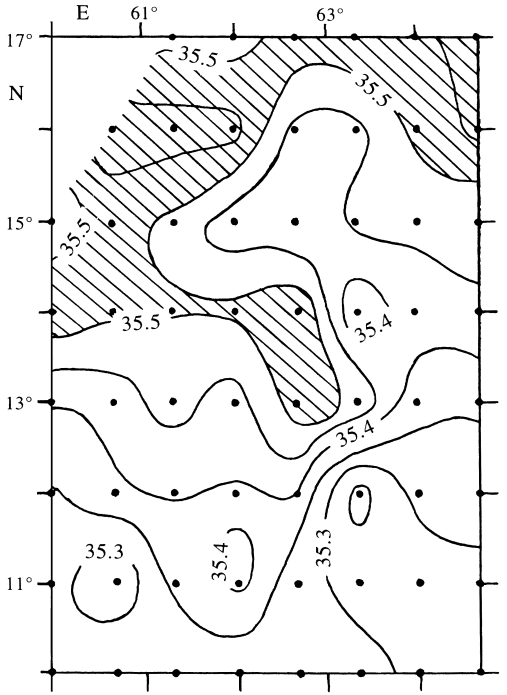

Fig. 3. Distribution of salinity on isopycnal surface $\sigma_t = 27.25\ kg \cdot m^{-3}$. Contour interval is 0.05. Area with $S > 35.5$ is shaded.

Density anomalies are small and positive: the maximum anomaly $\Delta\sigma_t$ between the lens core (St. 2600; 14°N, 62°40′E) and the background (St. 2642; 11°N, 62°40′E) is equal to $0.04\ kg \cdot m^{-3}$ at a depth of 700 m.

The CTD profile at St. 2600 indicates that the layer of maximum salinity ($S > 35.5$) related to the Reddy core covers the depth range 640–830 m (Fig. 5). The lens is characterized by a maximum temperature of 11.07°C and a maximum salinity of 35.56 with a corresponding density σ_t of $27.19\ kg \cdot m^{-3}$ at 665 m depth. Vertical profiles in the lens core (solid lines, Fig. 5) were compared both to mean profiles, calculated by averaging over 61 stations within the area 10–17°N, 60–64°40′E (dashed lines in Fig. 5), and to background profiles at St. 2642. Thermohaline anomalies in the Reddy reach maximum values of $\Delta S = 0.22$ and $\Delta T = 0.75$°C (at 800 m depth) compared to the background St. 2642.

Direct current measurements at three moorings located about 100 km south of the south-west corner of the CTD-survey (Fig. 1) show that velocities generally decrease with depth and do not exceed $5\ cm \cdot s^{-1}$ below 1500 m (Shchetinin *et al.*, 1981). For this reason, we chose the maximum depth of CTD measurements (1750 m) as a reference level for calculation of geostrophic currents within and around the Reddy. The map of dynamic topography at 700 m is displayed in Fig. 6. A narrow stream with maximum geostrophic velocity of more than $25\ cm \cdot s^{-1}$ near the ocean surface and of about

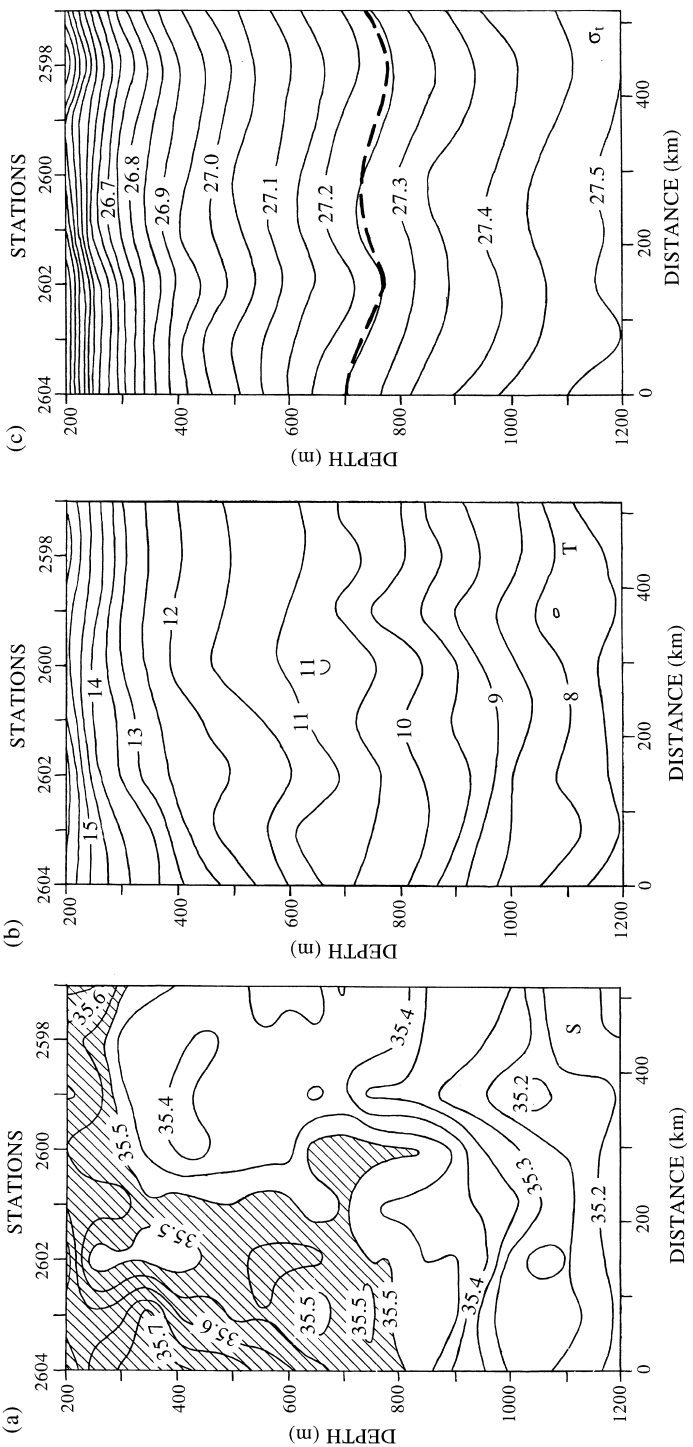

Fig. 4. Vertical sections of (a) salinity, (b) temperature (°C) and (c) density σ_t (kg·m^{-3}) along 14°N through the Reddy. Broken line indicates the neutral surface. Area with $S > 35.5$ is shaded.

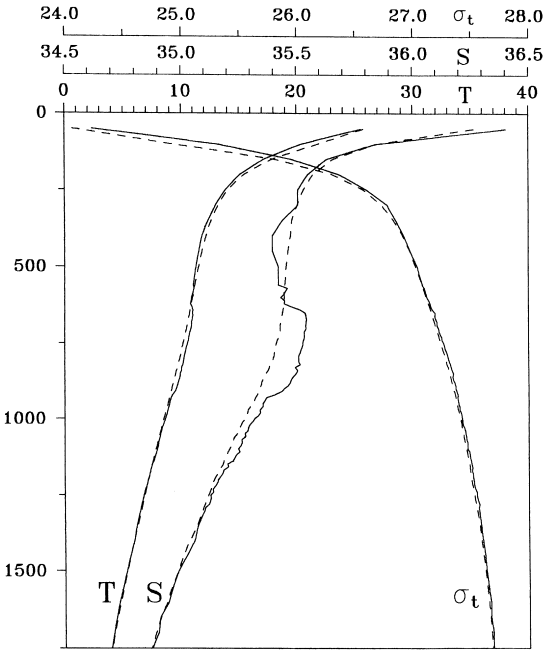

Fig. 5. Vertical profiles of temperature, salinity and density σ_t. Heavy lines denote profiles measured at St. 2600 (14°N, 62°40′E) in the Reddy; broken lines denote mean profiles calculated using data from 61 stations in the area 10–17°N and 60–64°40′E (see Fig. 2 for stations positions).

$10\,\mathrm{cm}\cdot\mathrm{s}^{-1}$ at 700 m depth crosses the map from south-west to north-east. This meandering flow corresponds to the leading edge of the main RSW tongue shown in Fig. 3 and probably belongs to the southern periphery of the large-scale cyclonic gyre occupying the northern part of the Arabian Sea (Wyrtki, 1971; Shchetinin *et al.*, 1981). A pair of vortices of opposite rotation is also evident in Fig. 6: an intensive anticyclonic eddy centred at 14–15°N, 64°E, and a cyclonic meander with peak-to-trough range of about 450–500 km. This vortex pair is observed at depths 0–1500 m, the geostrophic velocity of orbital rotation at 700 m reaches $12\,\mathrm{cm}\cdot\mathrm{s}^{-1}$.

Visual inspection of Figs. 3 and 6 reveals a linking of the Reddy to the synoptic-scale cyclonic meander. The normal component of geostrophic velocity on a section along 14°N through the meander and the embedded Reddy is represented in Fig. 7. Two jets with maximum speeds of more than $20\,\mathrm{cm}\cdot\mathrm{s}^{-1}$ in the subsurface layer and typical velocities up to $10\,\mathrm{cm}\cdot\mathrm{s}^{-1}$ below 600 m ($\sigma_t > 27.15\,\mathrm{kg}\cdot\mathrm{m}^{-3}$) display the meander position. The velocity component changes sign across the section on scale of about 200 km (positive values in Fig. 7 denote the northward flow). The presence of the warm and salty Reddy does not produce an opposite (anticyclonic) rotation of water at depths of 600–800 m, i.e. the vertical component of relative vorticity $\zeta = (\partial v/\partial x) - (\partial u/\partial y)$ does not change sign with depth. There is a net increase of cyclonic vorticity towards the ocean surface.

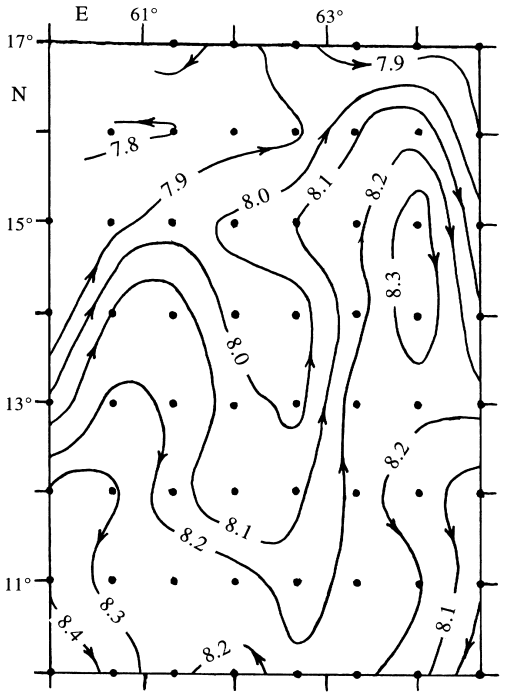

Fig. 6. Dynamic topography ($m^2 \cdot s^{-2}$) at 700 m relative to 1750 m.

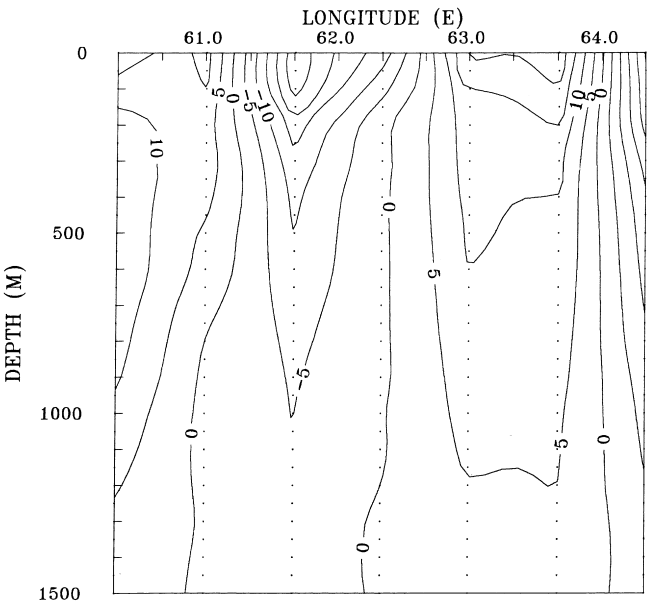

Fig. 7. Geostrophic velocity at 14°N. Contour interval is 5 $cm \cdot s^{-1}$. Positive flow is northward.

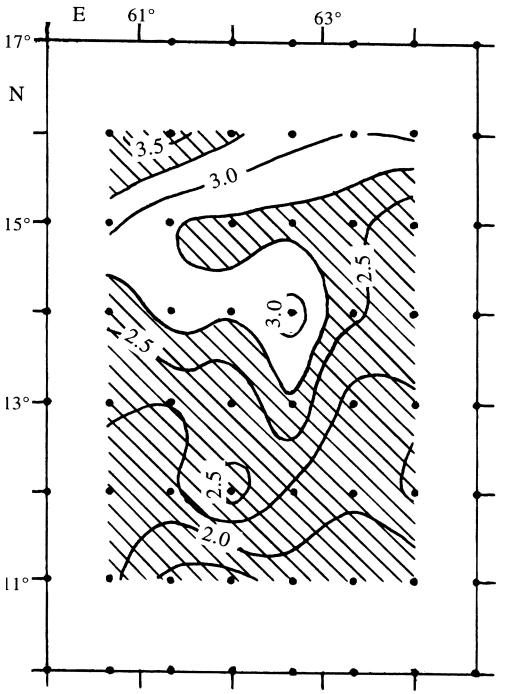

Fig. 8. Isopycnal potential vorticity IPV for the layer $\sigma_t = 27.15$–$27.35\ \mathrm{kg \cdot m^{-3}}$. Area with $2.75 \times 10^{-11} < IPV < 3.25 \times 10^{-11}\ \mathrm{m^{-1} \cdot s^{-1}}$ is unshaded.

A chart of isopycnal potential vorticity, $IPV = \frac{1}{\rho_0}\left(\frac{\partial v}{\partial x} - \frac{\partial u}{\partial y} + f\right)\frac{\mathrm{d}\sigma_t}{\mathrm{d}z}$ (here, f is the Coriolis parameter, ρ_0 the reference value of density), for the layer of $\sigma_t = 27.15$–$27.35\ \mathrm{kg \cdot m^{-3}}$ is shown in Fig. 8. The core of the Reddy is characterized by a relatively high ($3.1 \times 10^{-11}\ \mathrm{m^{-1} \cdot s^{-1}}$) value of IPV, which considerably exceeds the IPV values of the surrounding fluid. The main water mass with $IPV > 3.0 \times 10^{-11}\ \mathrm{m^{-1} \cdot s^{-1}}$ is located to the north-west of the along-frontal flow, in the region of predominant influence of RSW.

In order to use IPV as a Lagrangian property of a water parcel, we need to demonstrate that the diffusive mixing is small. The time scale for vertical mixing of the Reddy is estimated as $\tau = H^2/A$, where H is the Reddy thickness and A the effective (turbulent) diffusitivity. Substituting $H = 190\ \mathrm{m}$ and $A = 10^{-4}\ \mathrm{m^2 \cdot s^{-1}}$ one obtains $\tau \approx 11$ years. This means that diffusive mixing is negligible on time scale of lens formation (estimated as 1 month). As the IPV is a Lagrangian invariant in a water parcel, the spatial distribution of IPV shows that the Reddy comes from the north-western corner of the RSW tongue.

It was shown by McDougall (1984), McDougall (1987), that in a case of stable stratification the isentropic movement of a water parcel occurs along neutral surfaces.

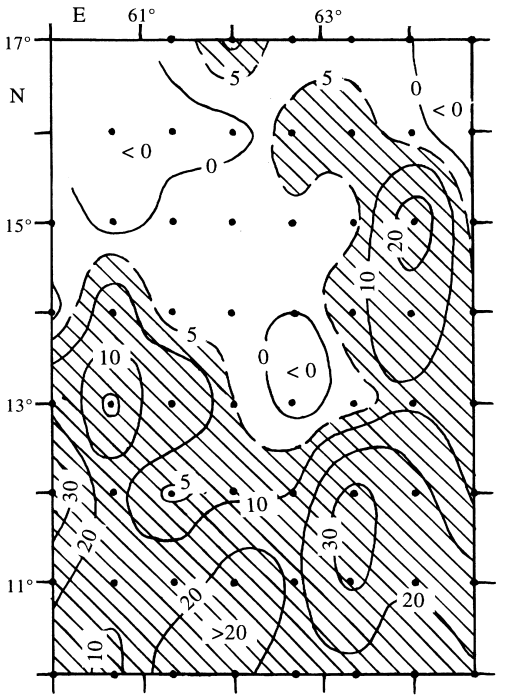

Fig. 9. Neutral surface deviation δh (m) from the $\sigma_t = 27.25\ \mathrm{kg \cdot m^{-3}}$ isopycnal surface. Area with $\delta h > 5$ m is shaded. The location of the neutral surface related to the Reddy core is shown by the broken line in Fig. 4c.

The position of a neutral surface in space is given by an equation $\rho(\vec{r}_0, \vec{r}) - \rho(\vec{r}, \vec{r}) = \sigma$ where $\rho(\vec{r}_0, \vec{r})$ is the *in situ* density of a water parcel moved from the point with $\vec{r}_0 = (x_0, y_0, z_0)$ to the point with $\vec{r}_0 = (x, y, z)$ coordinates, and $\rho(\vec{r}_0, \vec{r})$ is the background density in the point $\vec{r}$.

By analogy with Kostianoy and Shapiro (1989), it is possible to define the trajectory of the Reddy movement as a crossing line of the appropriate neutral and isopycnal surfaces. In our analysis we use σ_t surfaces, while σ_θ surfaces would be relevant. However, the difference between σ_t and σ_θ surfaces is small at the depth of the Reddy core and does not exceed 5 m. The location of the neutral surface related to the Reddy core is shown by the broken line in Fig. 4c. The vertical deviation δh (m) of the neutral surface from the $\sigma_t = 27.25\ \mathrm{kg \cdot m^{-3}}$ surface is shown in Fig. 9. It is clear from the above that the unshaded area with $\delta h < 5$ m (recall that the δh value of 5 m equals the maximum vertical resolution of our CTD measurements) is the "line" of these surfaces crossing, which indicates the trajectory of the Reddy motion.

Thus, two independent methods of determining the Reddy's trajectory and source region give similar results (see Figs. 3, 6, 8, and 9). We assert therefore that the point near 16°N, 61°E is the area where the dynamic impact of a synoptic-scale cyclonic meander on the large-scale tongue of RSW has resulted in the formation of a young Reddy.

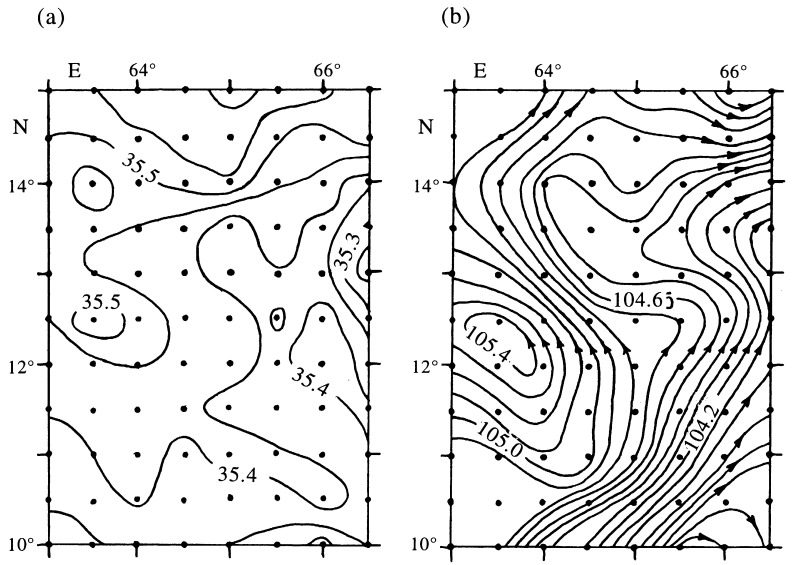

Fig. 10. Hydrographic data of the *POLYGON-67* experiment in the Arabian Sea (*R.V. Faddey Bellingshausen*, March–April 1967): (a) the salinity field on $\sigma_t = 27.25\,\mathrm{kg\cdot m^{-3}}$ isopycnal surface from SM (1991); (b) the dynamic topography of the ocean surface referred to 1500 m level from Koshlyakov *et al.* (1970).

3.1. Concluding remarks

The results of our study demonstrate that the formation of mesoscale lenses due to the influence of a meandering flow field on the RSW tongue occurs in the Indian Ocean. A deep-reaching cyclonic meander of a near-surface flow detached a semi-isolated patch of salty, warm water from the main RSW tongue and advected it away to the south for a distance of about 370 km. The dynamical signature is dominated by the cyclonic meander, and the Reddy is mainly a passive tracer. This mechanism of Reddy formation appears to be quite similar to the mechanism of Meddy formation in the Azores–Madeira region suggested by Käse and Zenk (1987).

A link of Reddies to synoptic-scale meanders (eddies) is apparently typical in the Arabian Sea. Mention should be made of another RSW lens found at 12°30′N, 63°30′E during the *POLYGON-67* experiment (March–April 1967, *R.V. Faddey Bellingshausen*). Reproduced from SM (1991), the distribution of salinity on the $\sigma_t = 27.25\,\mathrm{kg\cdot m^{-3}}$ isopycnal surface for the *POLYGON-67* experiment is represented in Fig. 10a. Comparison of Fig. 10a with a map of dynamic topography at the ocean surface (Fig. 10b) taken from Koshlyakov *et al.* (1970) shows that the position of the RSW lens practically coincides with the centre of an intensive cyclonic eddy.

A similar process of lens generation was observed by Shapiro and Emelianov (1989) in the Weddell-Scotia Confluence Zone, where the new lens was formed due to deep meandering of the southern branch of the Antarctic Circumpolar Current.

Acknowledgements

This work was supported by the Russian Foundation of Basic Research, Grant #94-05-17302 and ISF Grant JG7100. Fruitful discussions with Drs A.B. Polonsky, V.K. Kosnyrev, N.B. Shapiro and A.G. Zatsepin are acknowledged. We are grateful to Dr E.D. Barton for improving the English version of the manuscript.

References

Bower, A.S., Armi, L., Ambar, I., 1995. Direct evidence of Meddy formation off the south-western coast of Portugal. Deep-Sea Research I 42, 1621–1630.

Gamsakhurdia, G.R., Meschanov, S.L., Shapiro, G.I., 1991. On seasonal variability in the distribution of the Red Sea Water in the north-west Indian Ocean. Oceanologia 31, 47–54.

Käse, R.H., Zenk, W., 1987. Reconstructed Mediterranean salt lens trajectories. Journal of Physical Oceanography 17, 158–163.

Käse, R.H., Beckmann, A., Hinrichsen, H.-H., 1989. Observational evidence of salt lens formation in the Iberian Basin. Journal of Geophysical Research 94, 4905–4912.

Koshlyakov, M.N., Galerkin, L.I., Hien, C.D., 1970. On mesostructure of geostrophic currents in the open ocean. Oceanologia 10, 805–814.

Kostianoy, A.G., Shapiro, G.I., 1989. On the forecast of lens-like eddy trajectories in the ocean. Doklady Akademii Nauk SSSR 309, 1219–1222.

Maillard, C., Soliman, G., 1986. Hydrography of the Red Sea and exchanges with the Indian Ocean in summer. Oceanologica Acta 9, 249–269.

McDougall, T.J., 1984. The relative roles of diapycnal and isopycnal mixing on subsurface water mass conversion. Journal of Physical Oceanography 14, 1577–1589.

McDougall, T.J., 1987. Neutral surfaces in the ocean: implications for modelling. Geophysical Research Letters 14, 797–800.

Nof, D., 1982. On the movement of deep mesoscale eddies in the North Atlantic. Journal of Marine Research 40, 57–74.

Patzert, W.C., 1974. Volume and heat transport between the Red Sea and Gulf of Aden and notes of the Red Sea heat budget. In: L'oceanographie physique de la Mer Rouge, Cnexo, Paris, pp. 191–201.

Prater, M.D., Sanford, T.B., 1994. A Meddy off Cape St. Vincent Part I: Description. Journal of Physical Oceanography 24, 1572–1586.

Rochford, D.J., 1964. Salinity maxima in the upper 1000 meters of the north Indian Ocean. Australian Journal of Marine and Freshwater Research 15, 1–24.

Sabinin, K.D., 1964. The layers of high salinity in the North Indian Ocean. Trudy Instituta Okeanologii SSSR 64, 51–58.

Shapiro, G.I., 1984. The structure of a mesoscale vortex lens in the ocean thermocline. Doklady Akademii Nauk SSSR 276, 1477–1479.

Shapiro, G.I., Emelianov, M.V., 1989. Mesoscale hydrographic structure in the region of intense krill fishing in relation to chemical and biological properties of water masses. In: The Antarctic, Vol. 28, pp. 121–136. Nauka, Moscow (in Russian).

Shapiro, G.I., Meschanov, S.L., 1991. Distribution and spreading of Red Sea Water and salt lens formation in the northwest Indian Ocean. Deep-Sea Research 38, 21–34.

Shchetinin, Yu.T., Kosnyrev, V.K., Agafonov, E.A., Urdenko A.V., 1981. Oceanographic investigations in the north-western Indian Ocean in the spring–summer of 1980. In: Complex oceanographic investigations of the Indian Ocean, pp. 7–18. Marine Hydrophysical Institute, Sevastopol, (in Russian).

Wyrtki, K., 1971. Oceanographic Atlas of the International Indian Ocean Expedition, National Science Foundation, Washington, D.C., 531 pp.